

NeuPIMs: A NPU-PIM Heterogeneous Acceleration for Batched Inference of Large Language Model

Guseul Heo, Sangyeop Lee, Jaehong Cho, Hyunmin Choi, Sanghyeon Lee, Hyungkyu Ham, Gwangsun Kim, Divya Mahajan, Jongse Park

Abstract

Modern transformer-based Large Language Models (LLMs) are constructed with a series of decoder blocks. Each block comprises three key components: (1) QKV generation, (2) multi-head attention, and (3) feed-forward networks. In batched processing, QKV generation and feed-forward networks involve compute-intensive matrix-matrix multiplications (GEMM), while multi-head attention requires bandwidth-heavy matrix-vector multiplications (GEMV). Machine learning accelerators like TPUs or NPUs are proficient in handling GEMM but are less efficient for GEMV computations. Conversely, Processing-in-Memory (PIM) technology is tailored for efficient GEMV computation, while it lacks the computational power to effectively handle GEMM.

Inspired by this insight, we propose NeuPIMs, a heterogeneous accelerator-based system that jointly exploits a conventional GEMM-focused NPU and GEMV-optimized PIM devices. The main challenge in efficiently integrating NPU and PIM lies in enabling concurrent operations on both platforms, each addressing a specific kernel type. First, existing PIMs typically operate in a “blocked” mode, allowing only either NPU or PIM to be active at any given time. Second, the inherent dependencies between GEMM and GEMV in LLMs restrict their parallel processing. To tackle these challenges, NeuPIMs is equipped with *dual row buffers* in each bank, facilitating the simultaneous management of memory read/write operations and PIM commands. Further, NeuPIMs employs a runtime *sub-batch interleaving* technique to maximize concurrent execution, leveraging batch parallelism to allow two independent sub-batches to be pipelined within a single NeuPIMs node. Our evaluation demonstrates that compared to an NPU-only approach and a naïve NPU-PIM integrated system, NeuPIMs achieves 2.3× and 1.6× throughput improvement, respectively.

1 Introduction

Large Language Models (LLMs) are being widely deployed across various sectors such as natural language understanding [1–7], content generation [8–11], and decision support [12]. However, a key challenge with these models is the substantial resource requirement they impose - both memory and compute. This paper specifically addresses the inference challenges in contemporary LLMs, with an emphasis on models like GPT4 [1] and LLaMA [7].

The algorithmic commonality of these state-of-the-art LLMs is that their model architecture constitutes a stack of

decoder blocks. As illustrated in Figure 1(a), each block is structured around three primary layers: (1) Query-Key-Value (QKV) generation, (2) Multi-Head Attention (MHA), and (3) Feed-Forward Networks (FFNs). For efficient computation of these blocks, a prevalent strategy is batching multiple inference requests. Batching allows QKV generation and feed-forward layers to reuse weights across multiple requests, resulting in General Matrix Multiplication (GEMM) operations between weight and activation matrices. Conversely, the multi-head attention layer requires multiplication between activation matrices and activation vectors with no data reuse opportunity, leading to General Matrix-Vector Multiplication (GEMV) operations.

Overall, LLM inference involves the computation of numerous large-scale GEMMs and GEMVs. To address this computational demand, a common practice is to utilize high-performance machine learning (ML) accelerators, such as GPUs and TPUs. In this paper, we will refer to these ML accelerators as Neural Processing Units (NPUs). NPUs are often optimized for compute-intensive tasks, particularly for the efficient execution of GEMMs. However, their utility for GEMVs is less optimal due to the latter’s lower arithmetic intensity, which leads to under-utilization of the NPU’s computational resources. On the other hand, Processing-in-Memory (PIM) technology, while not as effective for GEMMs, shows promise for the bandwidth-intensive GEMV operations.

To this end, this work proposes NeuPIMs, a novel heterogeneous acceleration system for batched inference of LLMs. We architect NeuPIMs such that it effectively balances the utilization of memory bandwidth, computational resources, and memory capacity of the system to improve the overall inference throughput. NeuPIMs jointly exploits (1) a conventional GEMM-centric NPU using a 2D cluster of multiple systolic arrays and (2) a multitude of GEMV friendly processing-in-memory (PIM) accelerators. In designing NeuPIMs, we identify two major challenges:

- **Microarchitectural Challenge:** Current PIMs operate in a “blocked” mode, preventing the simultaneous execution of NPU and PIM. This serialization leads to an inherent under-utilization of resources.
- **Algorithmic Challenge:** In LLM decoder block, GEMM and GEMV operations have a data dependency. This algorithmic limitation fundamentally limits the possibility of parallel NPU-PIM computations.

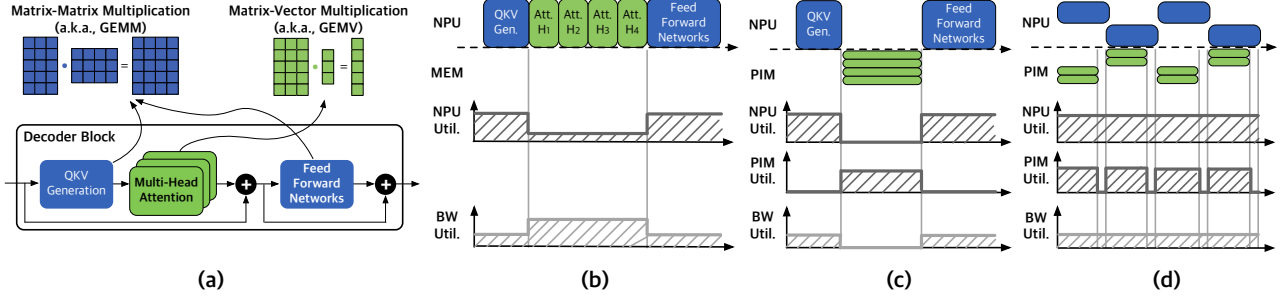


Figure 1. (a) Mathematical components of decoder blocks that constitute LLMs, (b) NPU-only baseline accelerator equipped with *non*-PIM memory (e.g., GPU), (c) NPU-PIM integrated baseline accelerator, and (d) the proposed NeuPIMs accelerator.

NeuPIMs addresses the aforementioned challenges by taking a hardware-algorithm co-design approach and makes the following contributions:

(1) Microarchitectural Contribution: To facilitate NPU-PIM parallel execution, NeuPIMs introduces a modified PIM bank architecture that enables regular memory accesses to occur concurrently with GEMV operations within the PIM. This is achieved by employing distinct row buffers for these two functionalities, hereafter referred to as *dual row buffers*. Dual row buffers leverage the property of DRAM where multiple rows can be activated independently without affecting functionality. This further requires handling and scheduling of mixed commands for memory access and PIM operation at the memory controllers without violating DRAM timing parameters. To do so, NeuPIMs strategically intersperses the two types of commands, minimizing row activation delays. Additionally, a few composite commands are appended to the baseline PIM ISA, performing multiple GEMV operations and thereby amortizing the controlling cost.

(2) Algorithmic Contribution: To enable parallel executions of GEMM and GEMV operators within the decoder block, we introduce the *sub-batch interleaving* technique, which concurrently processes two sub-batch inference computations on the NeuPIMs system. As the two sub-batches are independent of each other, it is possible to parallelize the execution of GEMM operations from one sub-batch with GEMV operations from another sub-batch. This approach creates avenues for simultaneous executions, enhancing overall efficiency. With sub-batch interleaving NeuPIMs aims to effectively balance the workload between GEMM and GEMV operations. To balance the pipeline of sub-batches, we estimate a table of mappings from sequence lengths to the MHA execution latency on the PIM. This information allows NeuPIMs to partition a given batch such that it balances the total sum of sequence lengths in the sub-batches.

Combining the proposed microarchitectural and algorithmic innovations, NeuPIMs achieves high utilization on both NPU and PIM accelerators, thus offering significant throughput improvement over NPU-only and naïve NPU-PIM

integrated baselines. Figure 1(b)-(d) visualizes the operator-accelerator mappings on NPU and/or PIM, along with their utilization trends for a short window in the execution runtime.

We evaluate the effectiveness of NeuPIMs using 3 variants of GPT3, a state-of-the-art LLM, with varying sizes. The evaluation utilizes real-world LLM inference datasets, ShareGPT and Alpaca, both accompanied by input and output sequence length information. We develop the NeuPIMs simulator by integrating well established SCALE-Sim [13] with a PIM simulator based on DRAMsim3 [14]. Our experimental results report that compared to an NPU-only and a naïve NPU-PIM integrated baseline accelerators, NeuPIMs achieves 2.3× and 1.6× throughput improvement, respectively. These significant throughput gains are attributed to the improved resource utilization of NPU and PIM from 39% and 18% to 57% and 22%, respectively. These compelling advantages highlight that NeuPIMs effectively overcome the limitations of existing solutions and take an effective initial step towards the practical deployment of PIM for LLM inference scenarios.

Remainder of the paper is organized as follows. Section 2 provides a background on the algorithmic foundations for batched execution of LLM inference. Section 3 presents the motivational analysis on GPUs, along with a discussion on potential alternatives. Section 4 concisely conveys the essence of proposed techniques, while Section 5 and Section 6 describe the microarchitectural and algorithmic techniques of NeuPIMs, respectively. Section 8.2 presents experimental results.

2 Background

2.1 Computational Characteristics of LLM Inference

Model architecture and execution of LLMs. Figure 2 illustrates the model architecture that all state-of-the-art large language models share [2, 6, 7, 15–17]. This illustration serves as a recurring example throughout the paper. For an input prompt (e.g., "I think this is"), the model undergoes an initiation phase, encoding the input to establish context for the subsequent generation phase. In the incremental phase, the model iteratively produces tokens one at a time, using the generated key-value projections as input for the next iteration. Both phases constitute a sequence of decoder blocks, each comprising three

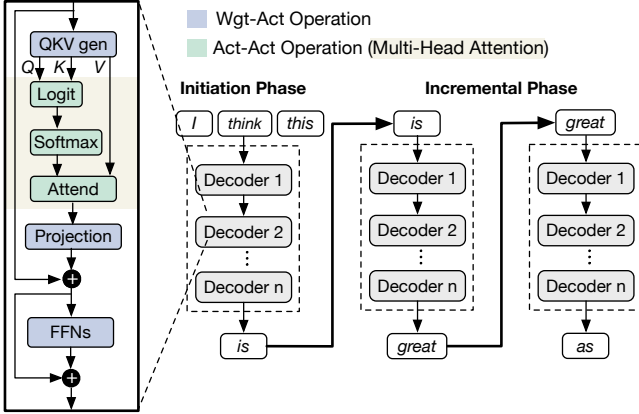


Figure 2. Model architecture and inference in LLMs.

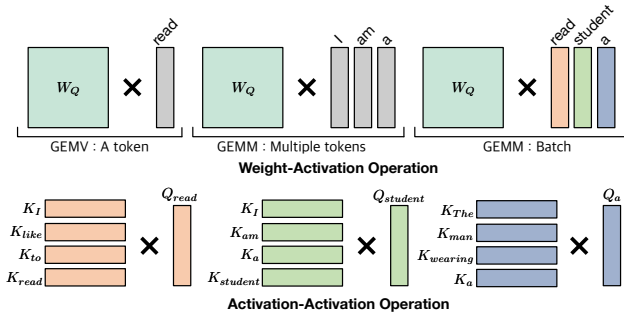


Figure 3. Operators in the attention layer.

major layers: (1) QKV generation, (2) multi-head attention (MHA), and (3) a set of feed-forward networks (FFNs).

Batched inference of LLMs. Computationally, the MHA layers have significantly different characteristics than QKV generation and FFN layers. Figure 3 denotes the example tensor operations of LLMs that show (1) weight-activation multiplications, and (2) activation-activation multiplications. The computations for QKV generation and FFNs are performed by multiplying a per-token Q/K/V activation or attention vector with the trained weight matrices (GEMV). However, these GEMV operators are transformed into GEMMs when (1) they are located at the decoders in the initialization phase, getting multiple token vectors in parallel (e.g., “I think this is”) or (2) multiple inferences are batched, further parallelizing the computations for multiple single-token generation processes. On the other hand, the computations for MHA layers are multiplications between two different activations where one is for the current token (vector), and the other is for all the tokens before this token (matrix), rendering a matrix-vector multiplication (GEMV). As the activation operands are unique for each inference request, their batching is not possible, making the computations highly memory bandwidth-bound.

Analysis of arithmetic intensity. To better understand the computational characteristics of LLM inference, we conduct a roofline analysis using two GPT3 variants, GPT3-13B and GPT3-175B. Figure 4 shows the relationship between the arithmetic intensity (FLOPS/byte) and performance

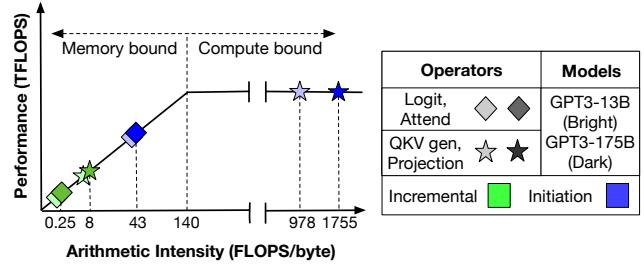


Figure 4. Arithmetic intensities of LLM layers.

(TFLOPS). We observe that for both models, the incremental phases are severely memory-bound, while the initialization phases are compute-bound. As these two phases have algorithmic dependencies and occur alternately in a sequential manner, it is fundamentally challenging to achieve high resource utilization using a homogeneous computing platform. This insight motivates this work and drives us to design a heterogeneous system that combines a compute-centric systolic array-based NPU for GEMMs with memory-centric Processing-in-Memory (PIM) accelerators for GEMVs.

2.2 LLM Inference Serving

As there is a massive resource demand for LLMs, the de-facto practice is to build a large-scale inference serving frameworks such as DeepSpeed [18] and vLLM [19]. These frameworks offer inference services for customer requests (i.e., prompts), which enables batching.

Selective batching. In general, batching is an effective method for neural network inference to improve resource utilization, while not sacrificing the latency requirement. However, MHA layers pose a challenge as they do not allow batching. This presents a difficulty for hyperscalers dealing with numerous customer requests while operating within limited compute resources. To address this, a recent work, Orca [20], proposes a solution where attention layers are individually computed, while QKV generation and FFN layers are batched. This approach allows the system to still benefit from batching when possible; otherwise, it serializes the computation. This unique algorithmic property necessitates the simultaneous computations of GEMM and GEMV, which is the main motivation for this work.

Iteration level scheduling. Inference serving system receives requests in a streaming fashion without a deterministic schedule. Therefore, there is a need for a parallelization approach that can efficiently process the non-deterministically collected set of inference requests. Orca [20] additionally proposes to schedule batched inference at the beginning of every incremental phase. This allows new inference requests to be added to and terminated requests to be removed from the batch. Consequently, newly arrived requests do not need to wait until the incremental phase for an already-started batch is terminated. This approach can significantly reduce the average latency for inference serving. NeuPIMs is built

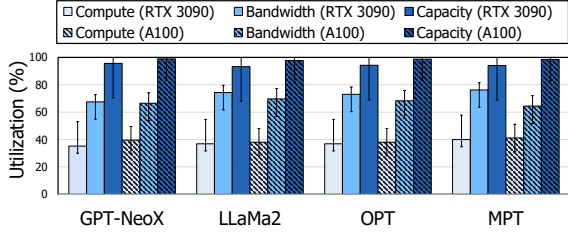


Figure 5. GPU resource utilization for four different LLMs.

upon this scheduling technique, and thus, it manages the inference requests at the iteration boundaries.

Memory paging for attention. vLLM [19] is another recent effort to enhance the resource utilization of LLM inference serving systems, with a specific focus on memory management. As discussed in Section 2.1, the QKV generation layer produces KV cache, the input for the attention layers that can be reused in the incremental phases. Leveraging this opportunity, LLM inference systems *cache* the KV projections in the memory, the size of which can be significant when the sequence length becomes large. vLLM introduces memory paging for this cached data, ensuring that a significant amount of memory is not pre-allocated long before its actual use. NeuPIMs employs the vLLM’s paging technique, implementing the page-based memory allocation mechanism for KV cache, which effectively increases the batch size significantly.

It is important to note that NeuPIMs is designed to be deployed on an inference serving system that incorporates all of these aforementioned techniques.

3 Motivation

This section provides the motivation that underlies the design decisions of NeuPIMs. First, we identify problems of the existing GPU-based LLM inference serving systems, which motivates the NPU-PIM heterogeneous approach. Then, we will discuss the limitations of naïve NPU-PIM integration approach, defining the target research challenges of this work.

3.1 GPU-based LLM Inference Serving

Particularly for LLMs, as they require a lot of memory, it is a common practice is to deploy them on a cluster of multiple GPUs [18, 21–24], leveraging pipeline parallelism [25, 26] and/or tensor parallelism [17, 27] to deploy the models.

Under-utilization of the GPU system. We analyze the state of the art GPU system to understand the utilization of compute, memory, bandwidth for LLM inference. We use NVIDIA A100 40GB GPU running four different LLM models: GPT-NeoX, LLaMa2, OPT, and MPT. Figure 5 presents the utilization results along with the layer-wise variations as error bars. The figure illustrates that while the capacity is not fully exploited due to inherent imperfections in parallelization schemes, it approaches 100%. This observation is intuitive as the number of GPUs in use is determined based on the capacity constraints. However, the utilization

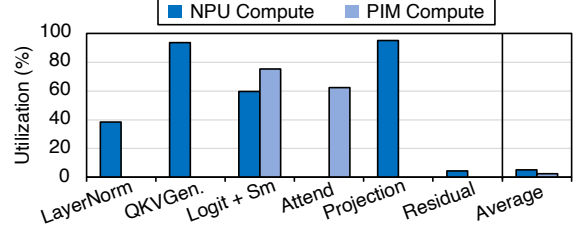


Figure 6. NPU-PIM resource utilization for decoder block.

of computational resources is consistently lower than 40%, which shows the cost-ineffectiveness of GPU-based LLM inference systems. We observe that this under-utilization is attributed to insufficient bandwidth, despite A100s being equipped with HBM providing an aggregate 1,555 GB/s. This imbalance is inevitable as long as serial dependencies between GEMMs and GEMVs persist. Moreover GEMVs are bandwidth-bound, further lowering the arithmetic intensity.

3.2 A Naïve NPU-PIM Approach

A straightforward approach to resolve this bandwidth bottleneck is to exploit the Processing-in-Memory (PIM) technology, which allows offloading the bandwidth-bound computations to its in-memory accelerator. Thus we design a naïvely integrated NPU-PIM accelerator, exploiting a systolic array architecture for the NPU and incorporating a state-of-the-art PIM-based GEMV accelerator, Newton [28]. We use the same methodology as in Section 3.1, where we replace GPUs with a standard NPU-PIM integrated design. The detailed hardware and system simulation methodology is described in Section 8. Figure 6 presents the computational resources and memory bandwidth utilization across different layers in the LLM decoder blocks. Overall, the utilization is significantly improved compared to the GPU counterpart. However, as different layers have different compute-bandwidth requirements, none of the layers lead to near-full utilization for both resources.

Necessity of concurrent NPU and PIM executions. The observed under-utilization is primarily due to the fundamental limitation in PIM’s microarchitecture that disallows the concurrent execution of host (NPU) and PIM units, which serializes the disjoint resource usage. Consequently, the most critical challenge in realizing the practical use of PIM in NPU accelerators is enabling their parallel executions. This research problem constitutes the focus of this work.

4 Overview of NeuPIMs

Figure 7 illustrates the overview of the proposed NeuPIMs system. This system alleviates the low resource utilization of an LLM inference serving system. To achieve this goal, NeuPIMs comprises: (1) an NPU equipped with systolic arrays and vector processing units, and multiple HBM-based PIM stacks that collaboratively process the batched inference requests, and (2) a scheduler that partitions an inference batch into two sub-batches and leverage sub-batch parallelism to

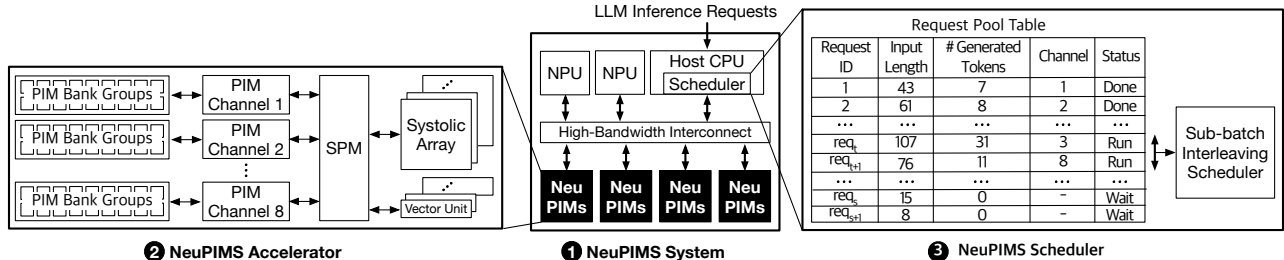


Figure 7. Overview of the proposed NeuPIMS system.

enable their interleaved executions for enhanced NPU-PIM parallelization (SW). Note, that the NeuPIMs NPU is a general representation of any machine learning accelerator such as TPU [29] and is not the contribution of this work. In this paper, we propose a novel system integrating PIM with NPU and the corresponding scheduling strategy. First, we provide an overview of the system.

1 NeuPIMs system. This system comprises a host CPU, multiple NeuPIMs stacks (NPU and PIM Accelerator), and multiple standalone NPUs connected through a high-bandwidth interconnect such as PCIe and CXL. As the initialization phase is entirely composed of GEMMs, we delegate its computation to the standalone NPUs, while NeuPIMs focuses on the computation of the incremental phase. While the diagram visualizes a single-node NeuPIMs, the system can scale to leverage tensor and pipeline parallelism, which is further discussed in Section 7. As in typical inference serving systems, our system receives the LLM inference requests in a streaming fashion. The requests are assigned to a PIM channel and queued in the request pool table until the on-going iteration is completed and a new iteration commences for the execution.

2 NeuPIMs’s PIM microarchitecture. We extend the design of standard PIM to support NeuPIMs LLM inferencing strategy. The bank architecture is expanded to include dual row buffers—one for PIM execution and the other for regular memory accesses, as illustrated in Figure 8. The dual row buffer architecture enables the NPU to perform memory read/write accesses on the bank rows that are not currently in use for PIM computations. This segregation is regulated by memory controllers to ensure that multiple activations are not issued over the same bank row (Section 5).

3 NeuPIMs scheduling algorithm. Our prototype NeuPIMs accelerator has 8 HBM-based PIM stacks, each of which is controlled by its own memory controller. The memory controllers manage the interleaving of memory read/write commands and PIM commands in a way that the inter-command timing delays are not violated, while maximizing the control path throughput. Effective interleaving is critical for performance since it is directly connected with the NPU and PIM concurrent executions (Section 6).

5 NeuPIMs Architecture

5.1 PIM Microarchitecture for Concurrent Execution

State-of-the-art single row buffer for PIM-based accelerator. Figure 8(a) depicts the high-level architecture of PIM-based GEMV accelerators that utilize banks equipped with a single row buffer. For a GEMV, the vector operand is first located in the global buffer shared across all banks in a channel. On the contrary, the rows of matrix operand are read from multiple banks simultaneously, exploiting bank-level parallelism, and located at their corresponding row buffers. When the operands are ready, the parallel multipliers and adder tree perform a partial dot-product by reading the broadcast vector input from the global buffer and per-bank row buffers.

Limitation of current PIM-based GEMV accelerators. Current PIM accelerators operate in a “blocked” mode, preventing the simultaneous execution of NPU and PIM. This limitation arises primarily because the memory bank utilizes a single row buffer that serves two purposes: read/write memory operations and PIM acceleration specifically for GEMV. These modes are managed sequentially, making it impossible to perform simultaneous parallelization. While this constraint does not significantly impact PIM system’s performance for sole execution of GEMV, it becomes pertinent for LLM conferencing that requires both GEMM and GEMV operations. Addressing this issue, our work aims to facilitate the parallel execution of both modes within the PIM framework. This advancement is expected to significantly enhance performance in LLM inferencing applications, unlocking the full potential of PIM beyond its current limitations.

Extending PIM with dual row buffers. Figure 8(b) delineates the microarchitecture of NeuPIMs bank. The memory banks of NeuPIMs are equipped with *dual row buffers*, namely MEM row buffer and PIM row buffer, which are associated with two independent data paths. Memory (MEM) row buffer is exclusively used for regular memory read/write accesses, whereas PIM row buffer is employed for GEMV operation. In designing NeuPIMs, our design principle is to minimize the microarchitectural modification since the complication would impose significant area and power costs, lowering the practicality in the real-world system. Instead, we delegate the complications to the command interface and memory control mechanism, which will be elaborated below.

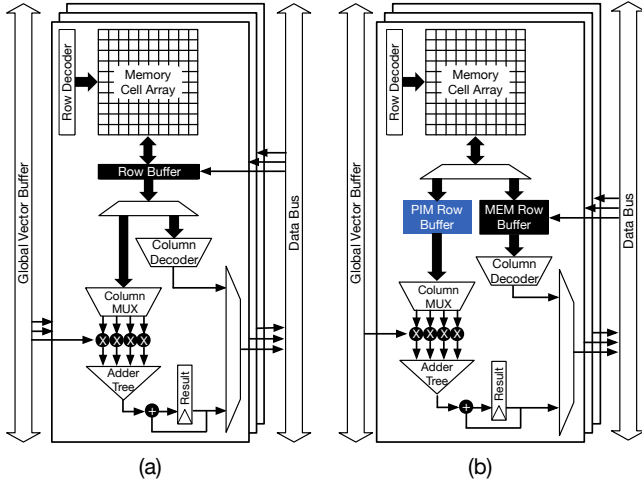


Figure 8. Microarchitecture of memory banks in (a) existing PIM accelerators with single row buffer banks, and (b) the proposed NeuPIMs with dual row buffer banks.

Table 1. List of NeuPIMs commands.

Command	Description
PIM_HEADER	Configure a GEMV operation
PIM_GEMV	Perform k multiplies and read the results
PIM_PRE	Precharge PIM row buffer

For prototyping and evaluating NeuPIMs, we choose an industry-developed PIM accelerator designed for GEMV, Newton [28]. However, note that the proposed techniques in this work are not bounded to the Newton architecture, rather applicable to any GEMV accelerator that follows the standard DRAM microarchitecture and command interface.

5.2 Memory Command Interface

Existing command interface for PIM-based GEMV. We build NeuPIMs on a PIM accelerator operated using a modified command interface on top of the existing DRAM standard interface. There are three commands that collaboratively operate the PIM. First, the host produces grouped activation commands, called “PIM_ACTIVATION”, which activate row buffers of multiple banks simultaneously, usually for 4 banks at a time due to the power constraints (i.e., tFAW). Once all the banks are activated, the host sends “PIM_COMPUTE” command that performs parallelized dot-product computation, extracting massively larger in-memory bandwidth than host-memory bandwidth. Finally, the “PIM_READRESULTS” command transfers the accumulated results to the host, ending a round of GEMV operation in PIM.

NeuPIMs command interface. We modify the command interface of baseline PIM by augmenting three additional commands that support new capabilities for NeuPIMs.

- **PIM_HEADER:** This command allows varying dimensionalities of GEMV operation. Existing PIM accelerators have a rigid architecture supporting a GEMV with fixed

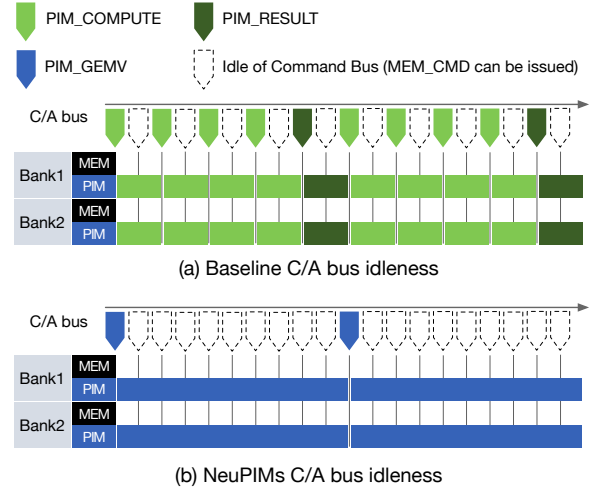


Figure 9. PIM command timing comparison.

dimensionalities, and therefore, the GEMV’s execution latency is deterministic. This property allows the memory controller to deterministically schedule the PIM commands without violating the DRAM refresh intervals. However, as NeuPIMs targets the GEMV operations of LLM’s MHA layers, its dimensionality varies depending on the sequence length, and thus, the memory controller has no means to accurately calculate the latency, which may lead to refreshment in the middle of PIM execution. To address this issue, NeuPIMs allows software to initialize a GEMV execution by sending the PIM_HEADER command, which delivers the dimensionality information of scheduled GEMV operation. This way, the memory controller is able to estimate the end-to-end latency of GEMV operation and schedule its constituent commands without conflicting with the memory refreshments.

- **PIM_GEMV:** The GEMV operation in existing PIM is controlled by a series of COMPUTE commands and the result is read using the READRES commands, as depicted in Figure 9(a). This fine-grained control approach naturally results in substantial command traffic. While this is not an issue for PIM that operates in a standalone mode, it becomes a significant concern for NeuPIMs that function in dual modes. PIM_GEMV is a composite command that controls multiple dot-products simultaneously, and at the end, returns the result back to the host NPU. Figure 9(b) shows an example timeline that shows the reduced command traffic by PIM_GEMV. The number of dot-products, k , is given as an argument for the command.
- **PIM_PRE:** As the NeuPIMs banks have dual row buffers, there is a need for an additional command that specifically precharges the PIM row buffers once the GEMV is completed. PIM_PRE is the same as the regular PRE command except that it triggers precharge of the PIM row buffer.

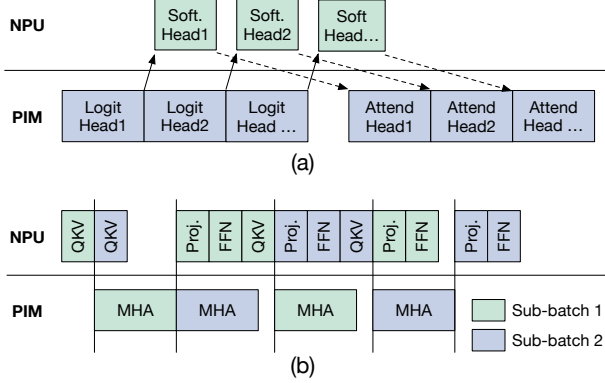


Figure 10. Example overlapping opportunity between (a) GEMV and consecutive softmax operations on NPU, and (b) Overview of sub-batch interleaving.

5.3 Memory Controller

For NeuPIMs, we have multiple channels, each of which has multiple PIM banks. The LLM requests are assigned to one of these channels, distributed across the multiple NeuPIMs accelerators. The memory controllers located in their respective PIN channels are equipped with their individual PIM command queues. PIM commands are broadcasted to all banks in the corresponding channel.

Interleaved scheduling of memory read/write and PIM commands. A challenge in the implementation of NeuPIMs memory controller is to interleave the memory read/write commands and PIM commands efficiently so that the command/address bus bandwidth does not become a performance bottleneck. NeuPIMs prioritize PIM commands over memory read/write commands, since the issuing delay of PIM commands is greater than that of memory commands, so the C/A bus bandwidth used to issue PIM commands is relatively small, allowing both commands to be issued without significant performance degradation.

6 NeuPIMs Scheduling

The integration of dual row buffers enables NeuPIMs to handle memory requests from NPUs and execute PIM commands simultaneously. To exploit the potential of the concurrent execution scheme of NeuPIMs, in this section, we provide a scheduling pipeline for multi-head attention in NeuPIMs and a novel batching technique named *sub-batch interleaving*.

6.1 NPU-PIM Overlapping Opportunities

Figure 10(a) illustrates the overlapping of head-granular logit, attend operations on PIM-side, and softmax operations on NPU-side in NeuPIMs. Since operations of multi-head attention can be decomposed to a head granularity, NPU-PIM integrated architecture has an opportunity to harness both resources to overlap operations. Naïve NPU-PIM integrated baseline cannot take advantage of this opportunity because operational results cannot be transferred between PIM units and vector units through PIM channels.

In contrast, NeuPIMs, by employing dual row buffers, can concurrently harness both NPU and PIM. This configuration allows vector units within NeuPIMs to access logit values without having to wait for the completion of the entire logit operations on the PIM, thereby reducing the underutilization of integrated units. Similarly, NeuPIMs eliminates the necessity to await the completion of the entire softmax operations on vector units, issuing PIM commands for each head to overlap attend operations efficiently.

6.2 Sub-batch Interleaving

To enhance the overall utilization of integrated units, sub-batch interleaving is employed, which involves dividing a large inference batch into two sub-batches. These sub-batches are then executed in an interleaved manner, and exploit the potential of dual row buffers. Figure 10(b) depicts the mapping process of each operation within the transformer decoder architecture to NeuPIMs. Each operation in the transformer decoder is mapped to optimize the utilization of the respective computational units in NeuPIMs. Multi-head attention, which primarily involves GEMVs, is assigned to PIM computation. In contrast, the remaining operations, such as QKV generation, Projection, and Feed Forward Networks, are mapped to the NPU part of NeuPIMs. These layers mainly consist of GEMMs, which favor systolic arrays to maximize wire-level data reuse.

For optimal exploitation of parallelism inherent in sub-batch interleaving, NeuPIMs must consider two key aspects: First, NeuPIMs requires a strategic balancing of the execution time for each sub-batch, particularly focusing on the multi-head attention. Since the latency of multi-head attention is determined by the channel processing the longest sequence, we must implement load balancing across the channels, ensuring an equitable distribution of token lengths. This challenge is addressed through a channel load balancing algorithm (Section 6.4). Second, NeuPIMs must ensure similar execution times for both sub-batches for efficient interleaved execution. The duration of each stage within the interleaving is bound by the processing time of more time-consuming sub-batch. For that, NeuPIMs introduces a sub-batch partitioning algorithm (Section 6.5).

6.3 Multi-Head Attention Latency Estimation

The latency of operations running in the NPU is largely dependent on the batch size of the inference. To apply optimization techniques for multi-head attention, we estimate the execution time of its operations by considering the key-value mapping to the PIM memory layout. Since the vector for GEMV is shared across the banks, the matrix for GEMV is interleaved row-wise to each banks. Consequently, key caches at the same row and column share the same layer and head index, with differing sequence indices. Conversely, value caches at the same row and column share the same layer, head, and sequence index, interleaving each head embedding

Algorithm 1: MHA Latency Estimation

Input: seq_len : Sequence length of the input request
Parameter: E : Model embedding size
 L_{tile} : GEMV latency for one PIM tile
 L_{Gwrite} : latency for writing one DRAM page
 E : Model embedding size
 P_{DRAM} : DRAM page size
 B_{chnl} : PIM banks per channel
 N_{head} : Number of heads
Output: L_{MHA} : Estimated latency for MHA

```
1  $L_{MHA} \leftarrow 0$ ;  
  /* GEMV latency for  $Key^T \times Query$  */  
2  $N_{tiles} \leftarrow (seq\_len / B_{channel}) * (E / P_{DRAM})$ ;  
3  $L_{MHA} += L_{Gwrite} * (E / P_{DRAM})$ ;  
4  $L_{MHA} += L_{Tile} * N_{tiles}$ ;  
  /* GEMV latency for  $Logits \times Value$  */  
5  $N_{tiles} \leftarrow ((E / N_{head}) / B_{chnl}) * ((seq\_len / P_{DRAM}) * N_{head})$ ;  
6  $L_{MHA} += L_{Gwrite} * ((seq\_len / P_{DRAM}) * N_{head})$ ;  
7  $L_{MHA} += L_{Tile} * N_{tiles}$ ;  
8 return  $L_{MHA}$ 
```

Algorithm 2: Channel Load Balancing

Input: L_{req} : A list for sequence length of new requests
 L_{chnl} : A list for request allocation of channels
/ Calculate each channel's total load by applying MHA latency estimation to each allocated request */*

```
1  $L_{load} \leftarrow []$ ;  
2 foreach  $chnl$  in  $L_{chnl}$  do  
3    $Sum_{load} \leftarrow 0$ ;  
4   foreach  $req$  in  $chnl$  do  
5      $Sum_{load} += MHALatencyEstimation(req)$   
6   end  
7    $L_{load}.append(Sum_{load})$ ;  
8 end  
  
  /* Allocate each request by greedy algorithm */  
9 foreach  $new\_req$  in  $L_{req}$  do  
10   $min\_index = Min(L_{load}).index()$ ;  
11   $L_{chnl}[min\_index].append(new\_req)$ ;  
12   $load_{req} = MHALatencyEstimation(new\_req)$ ;  
13   $L_{load}[min\_index] += load_{req}$ ;  
14 end  
15 return  $L_{chnl}$ 
```

into banks. Algorithm 1 takes this mapping into account to estimate the execution time of the multi-head attention latency.

6.4 Channel Load Balancing Algorithm

To minimize the execution time discrepancy between the most congested channel and the load-free channel, we developed the channel load balancing algorithm. Algorithm 2 leverages the aforementioned multi-head attention latency estimation to batch requests. It initially sorts the batch of requests in decreasing order of input token length. Then, NeuPIMs places a request with the longest token length in the channel

Algorithm 3: Sub-Batch Partitioning

Input: L_{req} : A list of active request set in each channel
Output: SB_1, SB_2 : Sub-batches for interleaving

```
1  $turn \leftarrow True$ ;  
2  $SB_1, SB_2 \leftarrow []$ ;  
3 foreach  $req_{chnl}$  in  $L_{req}$  do  
4    $size \leftarrow Size(req_{chnl}) \% 2$ ;  
5   if  $size \neq 0$  then  
6      $size = turn ? ceil(size) : floor(size)$ ;  
7      $turn = !turn$   
8   end  
9    $SB_1.append(req_{chnl}[size])$ ;  
10   $SB_2.append(req_{chnl}[size])$ ;  
11 end  
12 return  $SB_1, SB_2$ 
```

with minimal load. At each iteration, it updates the estimated latency, taking into account the newly appended request.

6.5 Sub-Batch Partitioning Algorithm

Given the dependency of NPU-friendly operations on the batch size of inference, it is essential to maintain a balanced size between the two sub-batches. As outlined in Algorithm 3, the approach involves dividing the requests for each channel into halves and appending each half to one of the sub-batches.

7 Scaling a NeuPIMs System

The standalone NPUs within the NeuPIMs node are dedicated to processing a request batch during the initiation phase, making full use of their computation units in the absence of the GEMV phase. Subsequently, after the initiation step, the generated key-value cache is transferred to the NeuPIMs node assigned to handle requests in the incremental phase. This approach attains high throughput by separating the two phases, each showcasing unique characteristics. In this section, we describe how NeuPIMs system adapts to models with varying parameter sizes without compromising the utilization of each hardware component. As for a single NeuPIMs, effectively maximizing throughput hinges on achieving a balance between NPU- and PIM-friendly operations. This concept is further applied to the entire system, where NeuPIMs strategically employs established parallelism techniques for LLMs [17, 22, 30] to ensure a harmonious workload distribution.

7.1 Tensor Parallelism with NeuPIMs

In the NeuPIMs system, tensor parallelism occurs within a single node, which consists of several NeuPIMs chips. Each operation that can be parallelized is divided into NPU-friendly operations and PIM-friendly operations. NPU operations, i.e., GEMMs are split based on already established partitioning strategy [17]. Tensor parallelism for PIM-friendly operations is straightforward. The operations can be divided at the head granularity, incurring no extra

Table 2. NeuPIMs hardware specification.

NPU Configuration	
Systolic Array Size	128x128
Vector Unit Size	128x1
Systolic Arrays / Chip	8
Vector Units / Chip	8
Channels / Chip	32
PIM Configuration	
Banks / Channel	32
Protocol	HBM2
Memory Capacity / Channel	1GB

capacity overheads. Note that, tensor parallelism strategy is not the contribution of this work, but this section highlights the adaptability of such techniques to NeuPIMs system.

Applying tensor parallelism yields two outcomes. First, each chip inside a node can allocate larger memory for key-value cache by distributing the weight for a model across several chips. The capacity required to store the key-value cache decreases proportionally to the number of chips per node, providing more headroom for a larger batch size. Increasing tensor parallelism effectively alleviates the compute intensity of NPU-friendly operations while increasing the overhead of PIM-friendly operations with a larger batch size. Tensor parallelism cannot continually increase due to the aggregation overhead associated with the growing number of chips per node. The network overhead is proportional to the product of batch size, the number of model layers, model embedding size, and the logarithm base 2 of the number of chips per node.

7.2 Pipeline Parallelism in NeuPIMs

NeuPIMs system also supports pipeline parallelism [25, 26]. With pipeline parallelism, each node alleviates the load of storing model weights. The size of the key-value cache per request per node also decreases proportionally to the number of pipeline parallelism since the layers of the model are distributed across the nodes. Thus, NeuPIMs can control the intensity of multi-head attention by increasing the available batch size, leveraging pipeline parallelism. The overhead from pipeline parallelism is transferring intermediate activations from one node to the next, and it is proportional to the size of the model embedding and the number of nodes.

8 Evaluation

8.1 Methodology

Cycle-level simulation. We build the NeuPIMs simulator on two open-source cycle-accurate simulators, SCALE-sim [13] and DRAMsim3 [14]. We linked the two simulators by modifying the memory interface of SCALE-Sim and offloading the memory accesses to the PIM simulator based on DRAMsim3.

Hardware specifications. We prototype NeuPIMs accelerator using a specific set of hardware specifications, which are listed in Table 2. Our NeuPIMs accelerator prototype is a multi-chiplet design containing 8 systolic arrays, each of which

Table 3. The evaluated LLM configurations.

Model	#Layers	#Heads	d_{model}	#TP	#PP
GPT3-7B	32	32	4096	4	1
GPT3-13B	40	40	5120	4	1
GPT3-30B	48	56	7168	4	2
GPT3-175B	96	96	12288	8	4

is equipped with 4 memory channels. Each systolic array is integrated with a SIMD vector unit that serves activation operations. Each memory channel controls 32 PIM banks, which offer in aggregate 1GB memory capacity. Note that while we choose this set of specifications for prototyping purposes, the NeuPIMs architecture is orthogonal to these choices, allowing varying configurations depending on the model size and data-specific properties (e.g., sequence lengths).

LLM models. We use three variants of GPT3, a state-of-the-art LLM developed by OpenAI as described in Table 3. While our experiments focus on GPT-3 model variants, NeuPIMs can host any decoder-based generation models, offering generality and wide applicability.

Baseline. For evaluation, we compare two baseline accelerators along with two NeuPIMs variants, namely NPU-only, NPU+PIM, NeuPIMs-DRB, and NeuPIMs-DRB+SBI.

- **NPU-only:** NPU-only represents existing NPU accelerators such as GPU and TPU, without any PIM capabilities. We assume that this baseline has the equivalent memory bandwidth with other alternatives for fairness. Moreover, a NPU is equipped with not only systolic array but also GPU-like vector processing units to generally support *non*-GEMM operators.
- **NPU+PIM:** NPU+PIM is a PIM-enabled NPU baseline, which integrates existing PIM-based GEMV accelerators with the off-the-shelf NPU accelerator. We merely map the GEMV operations in MHA layers to the PIM, while all the others are computed at the NPU side.
- **NeuPIMs-DRB:** NeuPIMs-DRB is a NeuPIMs accelerator only with the dual row buffer, lacking the sub-batch interleaving technique. To be fair, we assume that NeuPIMs-DRB employs a preliminary optimization of kernel fusion among MHA and Softmax layers.
- **NeuPIMs-DRB+SBI:** NeuPIMs-DRB+SBI is built upon the NeuPIMs-DRB, but also comes with the proposed scheduling technique, sub-batch interleaving, which in aggregate completes the design of NeuPIMs solution.

Datasets. We use two real-world LLM inferencing datasets, ShareGPT [31] and Alpaca [32]. ShareGPT dataset is a set of conversations scraped from the real-world user log of ChatGPT [33]. Alpaca dataset is an instruction dataset generated by OpenAI’s text-davinci-003 engine. The two datasets have distributions for input and output sequences. ShareGPT has an average input token length of 80 and an output of 296, while Alpaca has shorter sequence lengths of 12 and 56 for input and output, respectively.

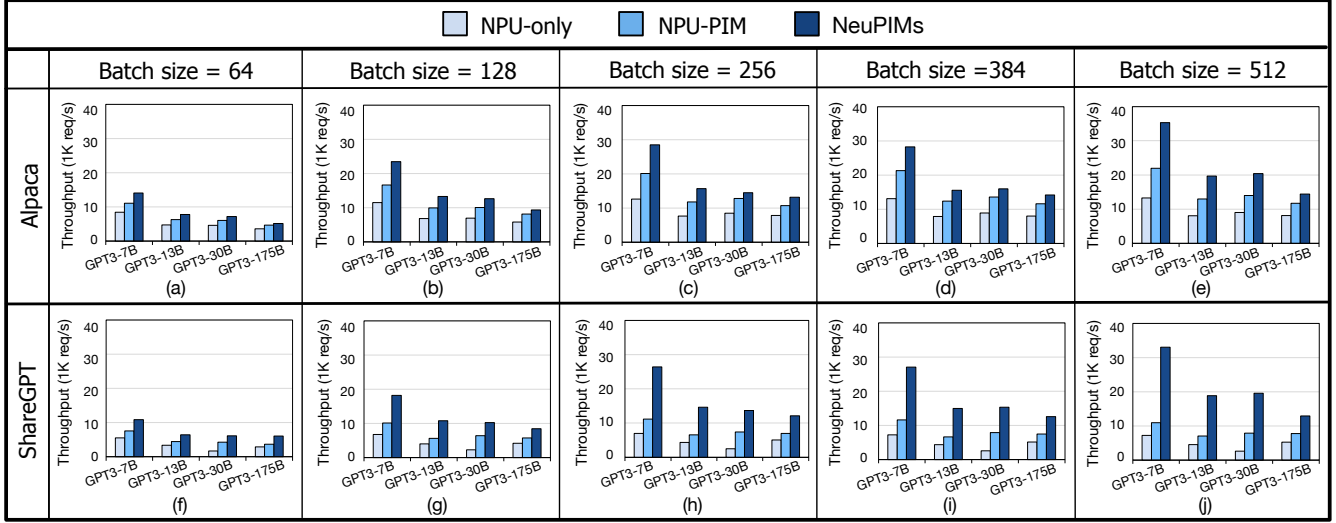


Figure 11. Throughput comparison results of NPU-only, NPU-PIM, and NeuPIMs. We use the two datasets, Alpaca and ShareGPT, using the batch sizes including 64, 128, 256, 384, and 512.

Workload. As running experiments for inference serving scenarios with a cycle-accurate simulator is infeasible, we develop an alternative methodology to synthesize workloads for system-level evaluation. To define the search space for workloads, we consider various hyperparameters, including model types, batch sizes, and tensor/pipeline parallelism. For each permutation of these hyperparameters, we simulate the inference serving for a fixed amount of time, randomly picking input prompts from the datasets. This way, we can warm up the inference batch in a way that the batch is filled with requests having various sequence lengths. We sample 10 different batches and use them to measure the throughputs of different hyperparameter combinations.

8.2 Results

Throughput. Figure 11 reports the throughput comparison results between the two baselines and NeuPIMs. Simply integrating PIM with the NPU, i.e., NPU-PIM already offers, on average 1.5 \times throughput improvement compared to the NPU-only baseline because the bandwidth-bound GEMV operations in MHA are all offloaded to the PIM. However, NeuPIMs consistently surpasses the NPU-PIM baseline, and offers *additional* throughput improvements over the NPU-PIM baseline across all the models and datasets, ranging from 10% to 3 \times . These trends are observed consistently for both datasets, with larger gains observed for ShareGPT, given its longer input/output sequences, offering increased acceleration opportunities for PIMs. Furthermore, as the batch size increases from 64 to 512, the throughput gains exhibit substantial growth. This is because the NeuPIMs system effectively shifts the bottleneck from bandwidth to compute towards the NPU, thus allowing NeuPIMs to extract higher performance

Table 4. Average resource utilization of NPU/PIM compute resource and memory bandwidth utilization.

	NPU-only	NPU-PIM	NeuPIMs
NPU	46.3%	38.5%	57.0%
PIM	-	17.9%	22.4%
Bandwidth	33.2%	36.1%	85.8%

from batched computation as the batch size grows. Note that NeuPIMs achieve significant throughput improvements using the same memory capacity, which demonstrates its cost-effectiveness, especially in a datacenter-scale inference serving scenario where larger batch sizes are advantageous.

Utilization. The main source of large throughput gain is the improved resource utilization across the board. Table 4 compares the average utilization for three major resources in the baselines and NeuPIMs, when using GPT3-13B, the batch size of 256, and the Alpaca dataset. As NPU-PIM delegates GEMV operation in MHA layers to PIM, it mitigates the bandwidth bottleneck, whereas the NPUs execute the GEMM operation, which decreases their compute utilization to 38.5% because the vector unit’s computation is migrated to PIM. However, NPU-PIM still suffers from temporal blocking due to the GEMM-GEMV dependencies in LLM inferencing. NeuPIMs overcomes this limitation, achieving 57% and 22% utilization on NPU and PIM, respectively, through the concurrent NPU-PIM execution capability. We observe similar trends from the other system configurations, which demonstrate the effectiveness of the proposed technique in enabling concurrent NPU-PIM execution by NeuPIMs.

Ablation study. Using NPU-PIM as the baseline, we augment the proposed three techniques and observe the performance behaviors, shown in Figure 12. For all batch sizes, the dual

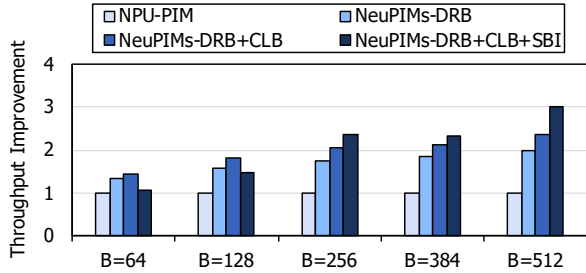


Figure 12. We use the GPT3-7B model and ShareGPT dataset for this experiment. DRB: Dual Row Buffers; CLB: Channel Load Balancing; SBI: Sub-Batch Interleaving.

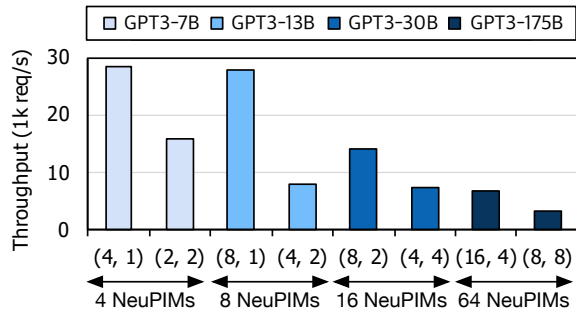


Figure 13. Throughput of multi-NeuPIMs system as the parallelization schemes change. We employ four combinations of tensor parallelism (TP) and pipeline parallelism (PP), represented as (TP, PP).

row buffers offer 69.7% throughput improvement on average, which has the largest impact on the performance as it enables concurrent NPU-PIM execution without significant overhead. The channel load balancing technique also always offers performance benefits by evenly distributing the requests to the available channels and, in turn, reducing the latency for performing the longest GEMV, which is on the critical path. In contrast to the previous two techniques, the sub-batch interleaving technique does not always yield gains. For small batch sizes, partitioning the batch into two may not sufficiently increase NPU compute utilization, and the penalty from pipelining could outweigh the benefits. However, when the batch size is equal to or larger than 256, NeuPIMs achieve the highest throughput, suggesting that batched inference with a large batch size is preferable for the NeuPIMs-based system.

Implication of parallelization schemes. As the LLM size increases, the NeuPIMs system must scale the number of devices to harness tensor and pipeline parallelisms. Figure 13 analyzes the implications of such parallelization schemes on the system throughput. For the experiment, we fix the total number of requests to 256, while the batch size per node varies depending on the parallelization scheme. The results highlight the preference for exploiting tensor parallelism over the pipeline counterpart, as it maintains a large batch size, resulting in better efficiency at the NPU. We observe this

trend consistently for all model variants, while the overall throughput decreases since the per-node batch size becomes small, due to low NPU utilization.

9 Related Work

LLM inference serving. Multiple LLM serving systems optimize for their inference performance either through reducing the memory footprint [34, 35], improving the kernel execution strategy [27], determining the partitioning techniques for intra- and inter-operator [17, 36, 37] execution, or a combination of these [18–21, 24, 30, 38]. In this work, we specifically tackle the utilization of the current hardware platforms which deploy these models through a compute and I/O suitable platforms, NPUs and PIMs, to create a more efficient system. Moreover, to ensure such a heterogeneous system can perform well for LLM inferencing, we offer a scheduling policy. Prior works that support kernel optimizations for better utilization of GPUs for LLMs, cannot fully mitigate the I/O and bandwidth bottleneck of GEMV kernels. Instead in this work, we build a system that can benefit from existing optimizations such as selective batching, KV caching, etc. to offer better utilization across the transformer model architecture.

PIM for language model support. TransPIM [39] proposes a new dataflow for transformer models to reduce the data loading latency during inference. This work accelerates the transformer operations on PIM and Near Memory Compute units. Instead, in this work, we enable the parallel execution of NPU and PIM to ensure a more balanced pipeline for LLM inference. AttAcc [40] further offers an accelerator (with PIM) for attention layer to reduce the data movement for the KV matrices. Instead NeuPIMs proposes a new system for PIM accelerator in addition to the scheduling of operations for the end to end inference of LLMs.

There are also variety of prior works that have leveraged PIM for GEMV operations [28, 41–46]. PIMs have been gaining a lot of attention due to their inherent potential in benefits towards bandwidth bound applications. However, none of these works enable simultaneous execution of PIM and NPU operations, necessary for the efficient execution of LLM inference.

Heterogeneous acceleration pipeline for deep learning. There are a variety of prior works that propose a pipelined solution for machine learning [47–49], however none of these prior works leverage PIM to alleviate the bandwidth requirement of LLMs. Certain prior works use an accelerator for specific models [50, 51], however, they do not alleviate the under-utilization of GEMV and GEMM operations in transformer decoder blocks.

10 Conclusion

Large Language Model (LLM) inferencing, given its significance, demands dedicated resources that can be deployed at scale. However, these models present a confluence of challenges, encompassing high memory capacity, high

compute intensity, and bandwidth constraints. In this work we propose a novel system, NeuPIMs, that integrates NPU (a general ML accelerator) with PIM technology to mitigate the limitations associated with different operations and their dataflow in the transformer layers. We introduce a novel scheduling and execution strategy for the proposed system, that can better utilize HBM memory, compute intensive NPU, and the PIM accelerator for LLM inference serving. Results indicate that the system developed in this work offers a 1.5× throughput improvement compared to the baseline system that naïvely integrates an NPU with the PIM accelerator.

References

- [1] OpenAI. Gpt-4 technical report, 2023.
- [2] Rohan Anil, Andrew M. Dai, Orhan Firat, Melvin Johnson, Dmitry Lepikhin, Alexandre Passos, Siamak Shakeri, Emanuel Taropa, Paige Bailey, Zhifeng Chen, Eric Chu, Jonathan H. Clark, Laurent El Shafey, Yanping Huang, Kathy Meier-Hellstern, Gaurav Mishra, Erica Moreira, Mark Omernick, Kevin Robinson, Sebastian Ruder, Yi Tay, Kefan Xiao, Yuanzhong Xu, Yujing Zhang, Gustavo Hernandez Abrego, Junwhan Ahn, Jacob Austin, Paul Barham, Jan Botha, James Bradbury, Siddhartha Brahma, Kevin Brooks, Michele Catasta, Yong Cheng, Colin Cherry, Christopher A. Choquette-Choo, Aakanksha Chowdhery, Clément Crepy, Shachi Dave, Mostafa Dehghani, Sunipa Dev, Jacob Devlin, Mark Diaz, Nan Du, Ethan Dyer, Vlad Feinberg, Fangxiaoyu Feng, Vlad Fienber, Markus Freitag, Xavier Garcia, Sebastian Gehrmann, Lucas Gonzalez, Guy Gur-Ari, Steven Hand, Hadi Hashemi, Le Hou, Joshua Howland, Andrea Hu, Jeffrey Hui, Jeremy Hurwitz, Michael Isard, Abe Ittycheriah, Matthew Jagielski, Wenhao Jia, Kathleen Kenealy, Maxim Krikun, Sneha Kudugunta, Chang Lan, Katherine Lee, Benjamin Lee, Eric Li, Music Li, Wei Li, YaGuang Li, Jian Li, Hyeontaek Lim, Hanzhao Lin, Zhongtao Liu, Frederick Liu, Marcello Maggioni, Aroma Mahendru, Joshua Maynez, Vedant Misra, Maysam Moussalem, Zachary Nado, John Nham, Eric Ni, Andrew Nystrom, Alicia Parrish, Marie Pellat, Martin Polacek, Alex Polozov, Reiner Pope, Siyuan Qiao, Emily Reif, Bryan Richter, Parker Riley, Alex Castro Ros, Aurko Roy, Brennan Saeta, Rajkumar Samuel, Renee Shelby, Ambrose Slone, Daniel Smilkov, David R. So, Daniel Sohn, Simon Tokumine, Dasha Valter, Vijay Vasudevan, Kiran Vodrahalli, Xuezhi Wang, Pidong Wang, Zirui Wang, Tao Wang, John Wieting, Yuhuai Wu, Kelvin Xu, Yunhan Xu, Linting Xue, Pengcheng Yin, Jiahui Yu, Qiao Zhang, Steven Zheng, Ce Zheng, Weikang Zhou, Denny Zhou, Slav Petrov, and Yonghui Wu. Palm 2 technical report, 2023.
- [3] Aohan Zeng, Xiao Liu, Zhengxiao Du, Zihan Wang, Hanyu Lai, Ming Ding, Zhuoyi Yang, Yifan Xu, Wendi Zheng, Xiao Xia, Weng Lam Tam, Zixuan Ma, Yufei Xue, Jidong Zhai, Wenguang Chen, Peng Zhang, Yuxiao Dong, and Jie Tang. Glm-130b: An open bilingual pre-trained model, 2023.
- [4] Jordan Hoffmann, Sebastian Borgeaud, Arthur Mensch, Elena Buchatskaya, Trevor Cai, Eliza Rutherford, Diego de Las Casas, Lisa Anne Hendricks, Johannes Welbl, Aidan Clark, Tom Hennigan, Eric Noland, Katie Millican, George van den Driessche, Bogdan Damoc, Aurelia Guy, Simon Osindero, Karen Simonyan, Erich Elsen, Jack W. Rae, Oriol Vinyals, and Laurent Sifre. Training compute-optimal large language models, 2022.
- [5] Sid Black, Stella Biderman, Eric Hallahan, Quentin Anthony, Leo Gao, Laurence Golding, Horace He, Connor Leahy, Kyle McDonell, Jason Phang, Michael Pieler, USVSN Sai Prashanth, Shivanshu Purohit, Laria Reynolds, Jonathan Tow, Ben Wang, and Samuel Weinbach. Gpt-neox-20b: An open-source autoregressive language model, 2022.
- [6] Susan Zhang, Stephen Roller, Naman Goyal, Mikel Artetxe, Moya Chen, Shuohui Chen, Christopher Dewan, Mona Diab, Xian Li, Xi Victoria Lin, Todor Mihaylov, Myle Ott, Sam Shleifer, Kurt Shuster, Daniel Simig, Punit Singh Koura, Anjali Sridhar, Tianlu Wang, and Luke Zettlemoyer. Opt: Open pre-trained transformer language models, 2022.
- [7] Hugo Touvron, Thibaut Lavril, Gautier Izacard, Xavier Martinet, Marie-Anne Lachaux, Timothée Lacroix, Baptiste Rozière, Naman Goyal, Eric Hambro, Faisal Azhar, Aurelien Rodriguez, Armand Joulin, Edouard Grave, and Guillaume Lample. Llama: Open and efficient foundation language models, 2023.
- [8] Aditya Ramesh, Prafulla Dhariwal, Alex Nichol, Casey Chu, and Mark Chen. Hierarchical text-conditional image generation with clip latents, 2022.
- [9] Mark Chen, Jerry Tworek, Heewoo Jun, Qiming Yuan, Henrique Ponde de Oliveira Pinto, Jared Kaplan, Harri Edwards, Yuri Burda, Nicholas Joseph, Greg Brockman, Alex Ray, Raul Puri, Gretchen Krueger, Michael Petrov, Heidy Khlaaf, Girish Sastry, Pamela Mishkin, Brooke Chan, Scott Gray, Nick Ryder, Mikhail Pavlov, Alethea Power, Lukasz Kaiser, Mohammad Bavarian, Clemens Winter, Philippe Tillet, Felipe Petroski Such, Dave Cummings, Matthias Plappert, Fotios Chantzis, Elizabeth Barnes, Ariel Herbert-Voss, William Hebgen Guss, Alex Nichol, Alex Paino, Nikolas Tezak, Jie Tang, Igor Babuschkin, Suchir Balaji, Shantanu Jain, William Saunders, Christopher Hesse, Andrew N. Carr, Jan Leike, Josh Achiam, Vedant Misra, Evan Morikawa, Alec Radford, Matthew Knight, Miles Brundage, Mira Murati, Katie Mayer, Peter Welinder, Bob McGrew, Dario Amodei, Sam McCandlish, Ilya Sutskever, and Wojciech Zaremba. Evaluating large language models trained on code, 2021.
- [10] Baptiste Rozière, Jonas Gehring, Fabian Gloeckle, Sten Sootla, Itai Gat, Xiaoqing Ellen Tan, Yossi Adi, Jingyu Liu, Tal Remez, Jérémy Rapin, Artyom Kozhevnikov, Ivan Evtimov, Joanna Bitton, Manish Bhatt, Cristian Canton Ferrer, Aaron Grattafiori, Wenhan Xiong, Alexandre Défossez, Jade Copet, Faisal Azhar, Hugo Touvron, Louis Martin, Nicolas Usunier, Thomas Scialom, and Gabriel Synnaeve. Code llama: Open foundation models for code, 2023.
- [11] Microsoft. Github copilot. <https://github.com/features/copilot>, 2022.
- [12] Shuang Li, Xavier Puig, Chris Paxton, Yilun Du, Clinton Wang, Linxi Fan, Tao Chen, De-An Huang, Ekin Akyürek, Anima Anandkumar, et al. Pre-trained language models for interactive decision-making. *Advances in Neural Information Processing Systems*, 35:31199–31212, 2022.
- [13] Ananda Samajdar, Jan Moritz Joseph, Yuhao Zhu, Paul Whatmough, Matthew Mattina, and Tushar Krishna. A Systematic Methodology for Characterizing Scalability of DNN Accelerators using SCALE-Sim. In *ISPASS*, 2020.
- [14] Shang Li, Zhiyuan Yang, Dhiraj Reddy, Ankur Srivastava, and Bruce Jacob. Drsim3: A cycle-accurate, thermal-capable dram simulator. *IEEE Computer Architecture Letters*, 19(2):106–109, 2020.
- [15] Jacob Devlin, Ming-Wei Chang, Kenton Lee, and Kristina Toutanova. BERT: Pre-training of Deep Bidirectional Transformers for Language Understanding. In *arXiv*, 2018.
- [16] MosaicML NLP Team. Introducing mpt-30b: Raising the bar for open-source foundation models, 2023. Accessed: 2023-06-22.
- [17] Nvidia. Megatron-lm. <https://github.com/NVIDIA/Megatron-LM>.
- [18] Reza Yazdani Aminabadi, Samyam Rajbhandari, Minjia Zhang, Ammar Ahmad Awan, Cheng Li, Du Li, Elton Zheng, Jeff Rasley, Shaden Smith, Olatunji Ruwase, and Yuxiong He. DeepSpeed Inference: Enabling Efficient Inference of Transformer Models at Unprecedented Scale. Technical report, Microsoft, 06 2022.
- [19] Woosuk Kwon, Zhuohan Li, Siyuan Zhuang, Ying Sheng, Lianmin Zheng, Cody Hao Yu, Joseph Gonzalez, Hao Zhang, and Ion Stoica. Efficient memory management for large language model serving with pagedattention. In *SOSP*, 2023.
- [20] Gyeong-In Yu, Joo Seong Jeong, Geon-Woo Kim, Soojeong Kim, and Byung-Gon Chun. Orca: A Distributed Serving System for Transformer-Based Generative Models. In *OSDI*, 2022.
- [21] NVIDIA. NVIDIA Triton. <https://developer.nvidia.com/triton-inference-server>, 2020.
- [22] Nvidia tensor rt 4.0. <https://developer.nvidia.com/tensorrt>.

- [23] ONNX Runtime developers. Onnx runtime. <https://onnxruntime.ai/>, 2021.
- [24] Huggingface. <https://github.com/huggingface/transformers/tree/main>, 2022.
- [25] Deepak Narayanan, Aaron Harlap, Amar Phanishayee, Vivek Seshadri, Nikhil R Devanur, Gregory R Ganger, Phillip B Gibbons, and Matei Zaharia. PipeDream: Generalized Pipeline Parallelism for DNN Training. In *Proceedings of the 27th ACM Symposium on Operating Systems Principles*, pages 1–15. ACM, 2019.
- [26] Yanping Huang, Youlong Cheng, Ankur Bapna, Orhan Firat, Dehao Chen, Mia Xu Chen, HyoukJoong Lee, Jiquan Ngiam, Quoc V. Le, Yonghui Wu, and Zhifeng Chen. GPipe: Efficient Training of Giant Neural Networks using Pipeline Parallelism. In *Advances in Neural Information Processing Systems 32: Annual Conference on Neural Information Processing Systems 2019, NeurIPS 2019, 8-14 December 2019, Vancouver, BC, Canada*, pages 103–112, 2019.
- [27] Lianmin Zheng, Zhuohan Li, Hao Zhang, Yonghao Zhuang, Zhifeng Chen, Yanping Huang, Yida Wang, Yuanzhong Xu, Danyang Zhuo, Eric P Xing, Joseph Gonzalez, and Ion Stoica. Alpa: Automating inter- and {Intra-Operator} parallelism for distributed deep learning. In *16th USENIX Symposium on Operating Systems Design and Implementation (OSDI 22)*, pages 559–578, 2022.
- [28] Mingxuan He, Choungki Song, Ilkon Kim, Chunseok Jeong, Seho Kim, Il Park, Mithuna Thottethodi, and T. N. Vijaykumar. Newton: A dram-maker’s accelerator-in-memory (aim) architecture for machine learning. In *2020 53rd Annual IEEE/ACM International Symposium on Microarchitecture (MICRO)*, pages 372–385, 2020.
- [29] Norm Jouppi, George Kurian, Sheng Li, Peter Ma, Rahul Nagarajan, Lifeng Nai, Nishant Patil, Suvinay Subramanian, Andy Swing, Brian Towles, Clifford Young, Xiang Zhou, Zongwei Zhou, and David A Patterson. Tpu v4: An optically reconfigurable supercomputer for machine learning with hardware support for embeddings. In *Proceedings of the 50th Annual International Symposium on Computer Architecture, ISCA ’23*, New York, NY, USA, 2023. Association for Computing Machinery.
- [30] Nvidia. Tensorrt-llm. <https://github.com/NVIDIA/TensorRT-LLM>.
- [31] ShareGPT Team. Sharegpt. <https://sharegpt.com>, 2023.
- [32] Rohan Taori, Ishaan Gulrajani, Tianyi Zhang, Yann Dubois, Xuechen Li, Carlos Guestrin, Percy Liang, and Tatsunori B. Hashimoto. Stanford alpaca: An instruction-following llama model. https://github.com/tatsu-lab/stanford_alpaca, 2023.
- [33] OpenAI. chatgpt. <https://chatgpt.com/blog/chatgpt>, 2023.
- [34] Xiaohui Wang, Ying Xiong, Yang Wei, Mingxuan Wang, and Lei Li. Lightseq: A high performance inference library for transformers, 2021.
- [35] Woosuk Kwon, Zhuohan Li, Siyuan Zhuang, Ying Sheng, Lianmin Zheng, Cody Hao Yu, Joseph Gonzalez, Hao Zhang, and Ion Stoica. Efficient memory management for large language model serving with pagedattention. In *Proceedings of the 29th Symposium on Operating Systems Principles, SOSP ’23*, page 611–626. New York, NY, USA, 2023. Association for Computing Machinery.
- [36] Jakub M Tarnawski, Amar Phanishayee, Nikhil Devanur, Divya Mahajan, and Fanny Nina Paravecino. Efficient algorithms for device placement of dnn graph operators. *Advances in Neural Information Processing Systems*, 33, 2020.
- [37] Reiner Pope, Sholto Douglas, Aakanksha Chowdhery, Jacob Devlin, James Bradbury, Anselm Levskaya, Jonathan Heek, Kefan Xiao, Shivani Agrawal, and Jeff Dean. Efficiently scaling transformer inference, 2022.
- [38] Christopher Olston, Noah Fiedel, Kiril Gorovoy, Jeremiah Harmsen, Li Lao, Fangwei Li, Vinu Rajashekhar, Sukriti Ramesh, and Jordan Soyke. Tensorflow-serving: Flexible, high-performance ML serving. *CoRR*, abs/1712.06139, 2017.
- [39] Minxuan Zhou, Weihong Xu, Jaeyoung Kang, and Tajana Rosing. Transpim: A memory-based acceleration via software-hardware co-design for transformer. In *2022 IEEE International Symposium on High-Performance Computer Architecture (HPCA)*, pages 1071–1085, 2022.
- [40] Jaewan Choi, Jaehyun Park, Kwanhee Kyung, Nam Sung Kim, and Jung Ho Ahn. Unleashing the potential of pim: Accelerating large batched inference of transformer-based generative models. *IEEE Computer Architecture Letters*, 22(2):113–116, 2023.
- [41] Jin Hyun Kim, Shin-haeng Kang, Sukhan Lee, Hyeonsu Kim, Woongjae Song, Yuhwan Ro, Seungwon Lee, David Wang, Hyunsung Shin, Bengseng Phuah, Jihyun Choi, Jinin So, YeonGon Cho, JoonHo Song, Jangseok Choi, Jeonghyeon Cho, Kyomin Sohn, Youngsoo Sohn, Kwangil Park, and Nam Sung Kim. Aquabolt-xl: Samsung hbm2-pim with in-memory processing for ml accelerators and beyond. In *2021 IEEE Hot Chips 33 Symposium (HCS)*, pages 1–26, 2021.
- [42] Seongju Lee, Kyuyoung Kim, Sanghoon Oh, Joonhong Park, Gimoon Hong, Dongyoon Ka, Kyudong Hwang, Jeongje Park, Kyeongpil Kang, Jungyeon Kim, Junyeol Jeon, Nahsung Kim, Yongkee Kwon, Kornijcuk Vladimir, Woojae Shin, Jongsoo Won, Minkyu Lee, Hyunha Joo, Haerang Choi, Jaewook Lee, Donguc Ko, Younggun Jun, Keewon Cho, Ilwoong Kim, Choungki Song, Chunseok Jeong, Daehan Kwon, Jieun Jang, Il Park, Junhyun Chun, and Joohwan Cho. A 1ynm 1.25v 8gb, 16gb/s/pin gddr6-based accelerator-in-memory supporting 1tflops mac operation and various activation functions for deep-learning applications. In *2022 IEEE International Solid-State Circuits Conference (ISSCC)*, volume 65, pages 1–3, 2022.
- [43] Jaehyun Park, Byeongho Kim, Sungmin Yun, Eojin Lee, Minsoo Rhu, and Jung Ho Ahn. Trim: Enhancing processor-memory interfaces with scalable tensor reduction in memory. In *MICRO-54: 54th Annual IEEE/ACM International Symposium on Microarchitecture, MICRO ’21*, page 268–281. New York, NY, USA, 2021. Association for Computing Machinery.
- [44] Sukhan Lee, Shin-haeng Kang, Jaehoon Lee, Hyeonsu Kim, Eojin Lee, Seungwoo Seo, Hosang Yoon, Seungwon Lee, Kyoungwan Lim, Hyunsung Shin, Jinhyun Kim, O Seongil, Anand Iyer, David Wang, Kyomin Sohn, and Nam Sung Kim. Hardware architecture and software stack for pim based on commercial dram technology : Industrial product. In *2021 ACM/IEEE 48th Annual International Symposium on Computer Architecture (ISCA)*, pages 43–56, 2021.
- [45] Youngeun Kwon, Yunjae Lee, and Minsoo Rhu. Tensordimm: A practical near-memory processing architecture for embeddings and tensor operations in deep learning. In *Proceedings of the 52nd Annual IEEE/ACM International Symposium on Microarchitecture, MICRO ’22*, page 740–753. New York, NY, USA, 2019. Association for Computing Machinery.
- [46] Xinfeng Xie, Zheng Liang, Peng Gu, Abanti Basak, Lei Deng, Ling Liang, Xing Hu, and Yuan Xie. Spacea: Sparse matrix vector multiplication on processing-in-memory accelerator. In *2021 IEEE International Symposium on High-Performance Computer Architecture (HPCA)*, pages 570–583, 2021.
- [47] Muhammad Adnan, Yassaman Ebrahimzadeh Maboud, Divya Mahajan, and Prashant J. Nair. Accelerating recommendation system training by leveraging popular choices. *Proc. VLDB Endow.*, 15(1):127–140, jan 2022.
- [48] Hardik Sharma, Jongse Park, Divya Mahajan, Emmanuel Amaro, Joon Kyung Kim, Chenkai Shao, Asit Misra, and Hadi Esmaeilzadeh. From high-level deep neural models to fpgas. In *MICRO*, October 2016.
- [49] Jongse Park, Hardik Sharma, Divya Mahajan, Joon Kyung Kim, Preston Olds, and Hadi Esmaeilzadeh. Scale-out acceleration for machine learning. In *MICRO*, October 2016.
- [50] Muhammad Adnan, Yassaman Ebrahimzadeh Maboud, Divya Mahajan, and Prashant J Nair. Heterogeneous acceleration pipeline for recommendation system training. *arXiv preprint arXiv:2204.05436*, 2022.
- [51] Youngeun Kwon and Minsoo Rhu. Training personalized recommendation systems from (gpu) scratch: Look forward not backwards. In *Proceedings of the 49th Annual International Symposium on Computer Architecture, ISCA ’22*, page 860–873. New York, NY, USA, 2022. Association for Computing Machinery.